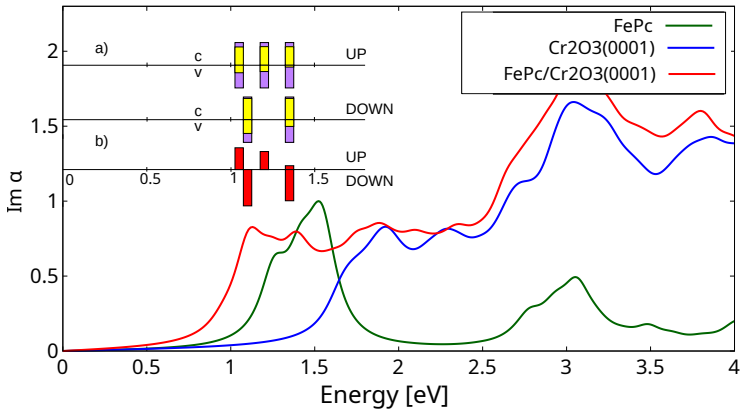


Figure 6.6 Optical absorption spectra (independent particle): polarizability of $Cr_2O_3$(0001) (blue), FePc/$Cr_2O_3$(0001) (red), and an FePc molecular layer such as in FePc/$Cr_2O_3$(0001) (green). The arbitrary units are chosen by normalizing the molecular peak at $\simeq$1.5 eV (green line) to 1. The transitions are broadened by $0.01$ eV. Bottom inset (b): the intensities (red) of the main transitions contributing to the FePc/$Cr_2O_3$(0001) spectrum in the spin-up (top) and spin-down (bottom) channels, normalized with respect to the largest one at $\simeq$1.1 eV. Only values greater than $10\%$ are shown. Top inset (a): the percentage of projection of the respective valence(bottom)/conduction(top) level on the molecule (yellow), characterizing the main transitions. An average of the in-plane directions has been considered.

to the top surface Cr1 atoms and to the top-bilayer Cr2-Cr3 atoms, and $z^{(c)} = 2.2$ Å, $0.5$ Å under the molecule, follow (as reported in Table 6.3). This analysis quantify the movement of charge from the top layers of the substrate toward the molecule.

Lastly, we can also investigate the Fe atom contribution to the above optical transitions; in fact, this could suggest a direct coupling between the optical excitation and the molecule magnetic momentum: a filling/emptying of the empty/filled d orbitals can produce a change in the Fe magnetic moment and so in the molecule magnetic moment. While the conduction states have a moderate Fe contribution in the spin up channel ($\simeq 1.4\%$) and in the spin down channel ($3-5\%$), the valence states have no contribution. A partial localization of the charge on the Fe atom can be supposed, which differ in the two spin channels, due to the larger intensity of the peaks in the spin-down channel; therefore, a decrease of the Fe magnetic moment can be suggested.

Table 6.2 Atoms average height. The top Cr1 layer height taken as the zero height.

| Atom | $z$ Å |
|---|---|
| Top Cr1 | $0.00$ |
| Top Cr2-Cr | $-1.40 \pm 0.13$ |
| Fe | $2.60$ |
| molecule | $2.70 \pm 0.2$ |

Table 6.3 Average height of the states contributing to the optical transitions at low energy for different spins: respectively, the valence ones $z^{(v)}$ and the conduction ones $z^{(c)}$. The top Cr1 layer height taken as the zero height.

| Spin | Energy | $z^{(v)}$ | $z^{(c)}$ |
|---|---|---|---|
| up | 1.09 | $-0.8$ | 1.4 |
| up | 1.24 | $-0.8$ | 1.4 |
| up | 1.37 | $-2.2$ | 1.4 |
| down | 1.11 | 0.1 | 2.1 |
| down | 1.38 | $-1.5$ | 2.1 |

## 6.6 Conclusions

From the studies of the FePc adsorption on the Cr2O3(0001) in its Cr-terminated configuration, the tendency of the molecule to bind through two of its imide N atoms and its phenyl-rings to the protruding surface Cr atoms emerges. Apart from local variations in the electronic and magnetic properties at the bonding points, and in proximity of the Fe atom, no significant effects are observed in the rest of the substrate. The optical spectrum analysis underlines that the adsorption of the molecule produces a breaking of the spin degeneracy in the optical excitations of the substrate. The appearance of substrate-molecule optical transitions than suggests the possibility to exploit the spinterface to couple the optical excitations and the spin excitations of the substrate.

CHAPTER 7

# Fe-phthalocyanine on $Cr_2O_3$(0001), O-terminated

In this chapter we study the FePc/$Cr_2O_3$(0001) O-terminated spinterface from an energetic, magnetic and optical point of view. This study is motivated by the collaboration with an experimental group (POLIMI) where such spinterface has been grown. With respect to the preceding spinterface, here the molecule disposes its molecular axis along the crystalline axis of the substrate and no strong bonding points apart from the Fe atom are observed. In spite of the weak binding, the effects on the substrate magnetic properties are significant and not only localized at the adsorption interface. In these terms, the O-terminated substrate is more magnetically reactive than the Cr-terminated one. This teaches us that the strongest binding does not necessarily involve the most significant changes in the substrate. The reactivity of the substrate is probably due to the major presence of O atoms at the top, and to the mainly ferromagnetic nature at the interface with the molecule.

## 7.1 Adsorption configurations

A deposition of 1 ML of FePc on the low coverage $Cr_2O_3$/Cu(110) surface is considered, as can be appreciated in the STM Fig. 7.1. Different regions are highlighted, Region 1 is the bare oxidized substrate of Cu(110), Region 2 is the FePc grown directly above Cu(110)-p(2x1)O, and Region 3 is the FePc grown on the $Cr_2O_3$ islands.

The missing of a long-range ordering in the FePc is as well confirmed by a DFT study of its adsorption configurations (Fig. 7.2), reported in Table 7.1. The configurations are distinguished by the angle between one of the molecular axis and one of the primitive surface axes $[2\bar{1}\bar{1}0]$, the position of the central Fe atom and the sign of its magnetic moment. Three Cr and two O atoms are visible from the top view, and are respectively differentiated by their relative height, normal to the surface. Going inward in the substrate we have O-up, Cr1, Cr2, Cr3 and O-down; of these Cr1 Cr2 and Cr3 are equally polarized. In addition, we call the O atom under the Fe atom Ob (b=below) and the O top layer Oa (a=average).

The adsorption energies for the different configurations are reported in Table 7.1.

As reference for the isolated molecule configuration, the Jahn-Teller configuration is considered, $D_{2h}$, with a difference in the non-equivalent Fe-N bonds of $0.1\%$, as already emphasized previously. As expected, between the different configurations not significant energy differences, justifying the missing in-plane ordering. Although, a preference for the adsorption on the O sites can be observed, with a difference of $0.43$ eV between the two minimal ones. The similarity between the Cr configurations is due to the fact that these centers differ only slightly in the their respective height. The preference for the rotated configuration reminds the tendency of the imide N atoms to bond to the Cr

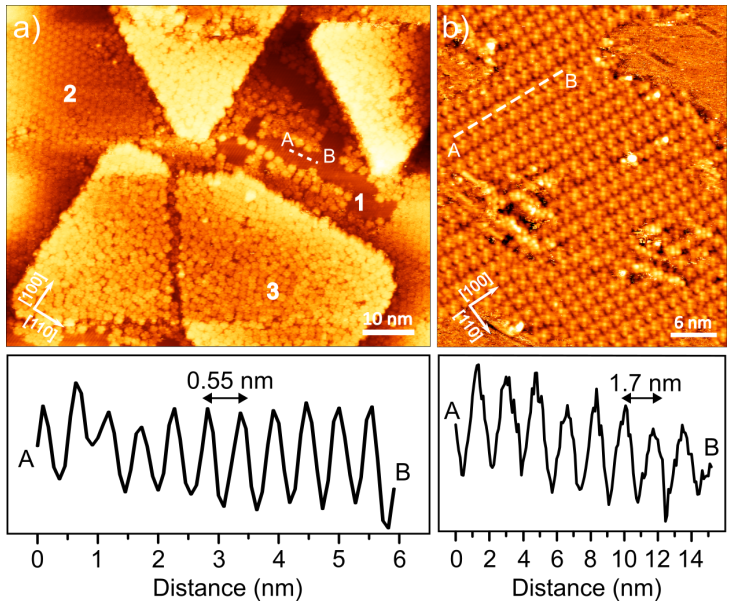


Figure 7.1 a) STM image of 1 ML of FePc on $Cr_2O_3$/Cu(110); size 90 × 90 nm$^2$, setpoint $\Delta V$ = -2.8 V $I$ = 0.1 nA. b) Zoom on the FePc/Cu(110) region; size 50 × 50 nm$^2$, setpoint $\Delta V$ = -1.5 V, $I$ = 0.2 nA. The graphs below each STM image report the corrugation profiles taken along the corresponding AB dashed lines. The shown directions refer to the Cu(110) substrate. Credits: Alberto Brambilla et collaborators, POLIMI.

Table 7.1 Adsorption energy of the considered configurations, in the ferromagnetic (FM) and antiferromagnetic (AF) alignment between Fe and topmost Cr atoms.

| Site | Angle | $E_{ads}^{FM}$ (eV) | $E_{ads}^{AF}$ (eV) | $E_{ads}^{AF} - E_{ads}^{FM}$ (eV) |
|---|---|---|---|---|
| Cr1 | 0° | -3.992 | -4.010 | -0.018 |
| | 45° | -4.085 | -4.105 | -0.020 |
| Cr2 | 0° | -3.987 | -4.020 | -0.033 |
| | 45° | -4.114 | -4.137 | -0.023 |
| Cr3 | 0° | -4.066 | -4.105 | -0.039 |
| | 45° | -4.185 | -4.220 | -0.035 |
| O-up | 0° | unstable | -4.314 | |
| | 15° | -4.419 | -4.462 | -0.043 |
| | 30° | -4.633 | -4.644 | -0.044 |
| | 45° | -4.502 | -4.548 | -0.047 |
| O-dn | 0° | -4.084 | -4.107 | -0.023 |
| | 30° | unstable | -4.101 | |
| | 45° | -4.063 | -4.079 | -0.017 |

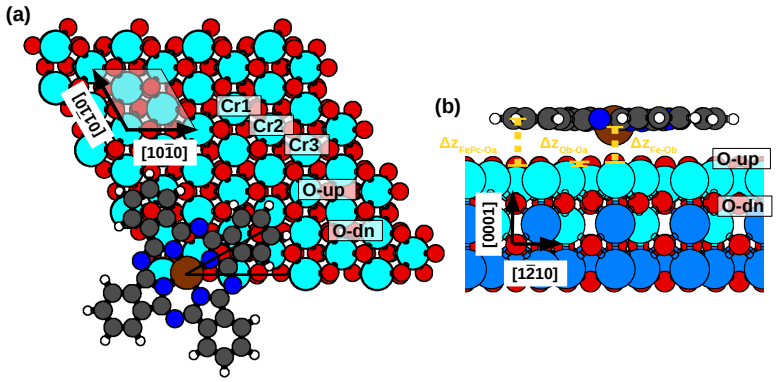


Figure 7.2 (a) Top view of the relaxed minimum adsorption energy configuration (O-up 30° FM) of the FePc/$Cr_2O_3$(0001) spinterface, indicating the angle between the N-Fe-N axis and the surface $[10\bar{1}0]$ direction and the unit cell. (b) Its side view, indicating in yellow, respectively, the distance molecule (excluding the Fe atom) O-up layer ($\Delta z_{\text{FePc-Oa}}$), the distance Fe O-up atom underneath ($\Delta z_{\text{Fe-Ob}}$), and the distance of the latter O-up atom and the O-up layer $\Delta z_{\text{Ob-Oa}}$. Color scheme as follows: light and dark blue: Cr according to their respective magnetization; red: O; brown, Fe; dark blue, N; gray, C; white: H. The names of the adsorption sites are directly indicated. In particular, the three Cr and two O atoms as visible from a top-view of the surface are differentiated by their respective height, normal to the surface: from top to bottom, O-up, Cr1, Cr2, Cr3, and O-down.

atoms of the Cr-terminated surface (see Chapter 6), here however the effect is less significant due to the fact that the Cr atoms are now sub-surface and not protruding. In the O configurations, the same preference can be observed as well. This tendency of the molecule to have one of its axis along the crystalline direction $[\bar{1}2\bar{1}0]$, can then be partially explained trough the N-Cr similar-bonding, and trough the C-O bonding, as the rotated configurations maximise the overlap between the C and O atoms. These two explanations are mainly motivated by the studies of the variations in the magnetic moments and electronic charges, as these atoms are the mostly affected ones.

For what concerns the magnetic ordering, AF ordering is the preferential one, and is justified by the super-exchange mechanism mediated by the O atoms. This is as expected from similar results on NiO(001) (Chapter 8) and CoO(001) (Chapter 4). The energy difference between the FM and AF configurations of the molecule is typically below $50$ meV. This result is in agreement with the XMCD results in Fig. 7.3, which underline a magnetic ordering of the molecule at the surface, and for normal incidence and for $45°$ incidence. However, in order to have a magnetic ordering of the molecule, an AF coupling with the substrate is not sufficient, but the spot observed through the XMCD must correspond to the same magnetic domain. In some way the issue is self-consistent: observing a molecule magnetic ordering and knowing that the molecule-substrate coupling is mainly AF, we are observing the same magnetic domain of the substrate; with respect to which the molecules are magnetically ordered.

From a structural point of view, in the different configurations the height of the Fe atom is lower than that of the rest of the molecule. However, while in the Cr1 and Cr2 configurations the difference is around $0.1$ Å and the molecule preserves a flat geometry

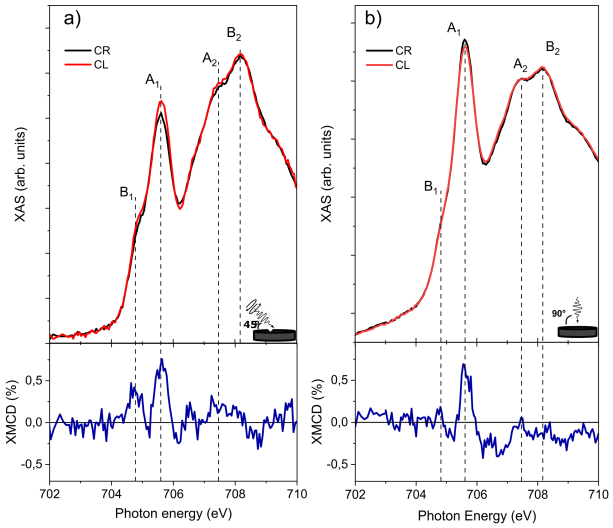


Figure 7.3 XMCD spectra acquired on FePc/$Cr_2O_3$/Cu(110) at a) $\theta = 45°$ (grazing incidence), and b) $\theta = 90°$ (normal incidence). Credits: Alberto Brambilla et collaborators, POLIMI.

(the distance of the molecule from the average O-up layer is $\Delta z_{\text{FePc-Oa}} = 2.8 - 3.0$ Å), in the other configurations the difference is larger, and the atoms around the Fe atom are partially dragged towards the surface. In detail, in the Cr3 configurations the Fe atom height is $\Delta z_{\text{Fe-Oa}} = 2.6$ Å, with a difference with respect to the the rest of the molecule of $0.3$ Å; in the O-dn configurations $\Delta z_{\text{Fe-Oa}} = 2.7 - 2.8$ Å, with a difference of $0.2$ Å; and in the O-up configurations $\Delta z_{\text{Fe-Oa}} = 2.4$ Å, with a difference of $0.4$ Å (with the exception of the O-up at $0°$ with $\Delta z_{\text{Fe-Oa}} = 2.7$ Å and a difference of 0.2 Å). The surrounding pyridinic N atoms are partially dragged ($2.7 - 2.9$ Å) towards the surface, being $0.04$ Å lower on average than the imide ones ($0.10$ Å in the O-up configurations). Comparing these results with the adsorption energies (Tab. 7.1), a reduction in the latter can be associated to the lowering of the Fe atom towards the O-up atoms of the surface, as observed in Co(001) and Ni(001). In the most stable O-up configuration at $30°$, the Fe atom chemically bonds with the top O-up atom below ($\Delta z_{\text{Fe-Ob}} = 2.25$ Å), that in turn is lifted by $\Delta z_{\text{Ob-Oa}} = 0.15$ Å over the O layer of the substrate, see Fig. 7.1 (b).

However, we remeber that the Fe atom height differences are not sufficient to explain the energy variations between the different angles; which requires, instead, the study also of the rest of the molecule as testified by the analysis as a function of the molecular angle.

## 7.2 Electronic properties

We can in detail study the electronic properties of the minimum adsorption energy configuration, looking at its PDOS Fig. 7.4.

The molecular orbitals hybridize with the substrate states, as they shift in energy and

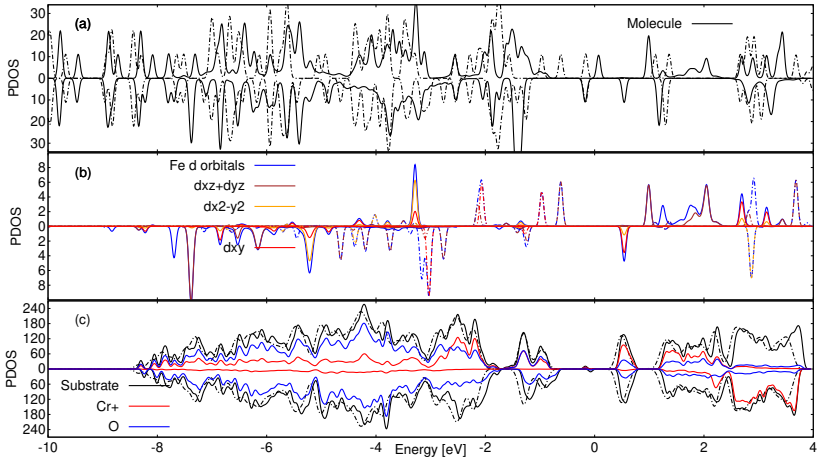


Figure 7.4 Electronic PDOS of FePc/$Cr_2O_3$(0001), summed over: (a) all molecule atoms; (b) Fe d-orbitals; (c) substrate atoms. Substrate color codes: black = all substrate atoms; red = Cr atoms of one spin component ("Cr+", $d$ orbitals); blue = all O atoms. Solid/dash-dotted lines indicate adsorbed and gas phase molecules or pristine substrate, respectively. Negative spin components are shown as negative values. All values in states/eV/cell.

broaden. As a consequence, a reduction of the band gap of the full system, with respect to the free molecule or pristine substrate one, can be observed: $1.34 \rightarrow 0.24$ eV in the spin-up channel and $1.33 \rightarrow 0.53$ eV in the spin-down channel. In the spin-up channel, the highest valence state (located at $0.17$ eV below the Fermi energy as seen in Fig. 7.4) is of substrate nature, while the lowest conduction state is of molecular nature. In the spin-down channel, instead, the lowest conduction state and the highest valence state (located at $0.07$ eV below the Fermi energy) are both of substrate nature.

However, looking at the Fe d orbitals (Fig. 7.4 (b)), a shift and broadening of the energy levels is not sufficient to explain the variations observed after the adsorption. Indeed, the molecule undergoes a spin-crossover: two electrons populating the $d_{xz} + d_{yz}$ and the $d_{xy}$ orbitals in the spin-up channel (minority channel) move to the $d_{x^2-y^2} + d_{z^2}$ orbitals in the spin-up and spin-down channels (majority channel). The absolute value of the Fe magnetic moment, thus, changes going from $-2.17\mu_B$ to $-3.08\mu_B$. The orbital configuration of the Fe ion, as well, changes from $d^{\downarrow}_{z^2} d^{\downarrow}_{xz} d^{\uparrow\downarrow}_{yz} d^{\uparrow}_{xy} d^{\downarrow}_{xy}$ to $d^{\downarrow}_{z^2} d^{\downarrow}_{xz} d^{\downarrow}_{yz} d^{0.6\downarrow}_{xy} d^{0.4\uparrow}_{xy} d^{\uparrow}_{x^2-y^2} d^{\downarrow}_{x^2-y^2}$.

## 7.3 Magnetic properties

In Figs. 7.5- 7.6 the spin density and electronic charge density variations of the minimum adsorption energy configuration with respect to the pristine system and isolated molecule are reported, respectively projected on a plane cutting through the substrate and along the interface. These variations are computed as the differences in the Lowdin populations.

While from a top-view it seems that the substrate is affected by the adsorption of

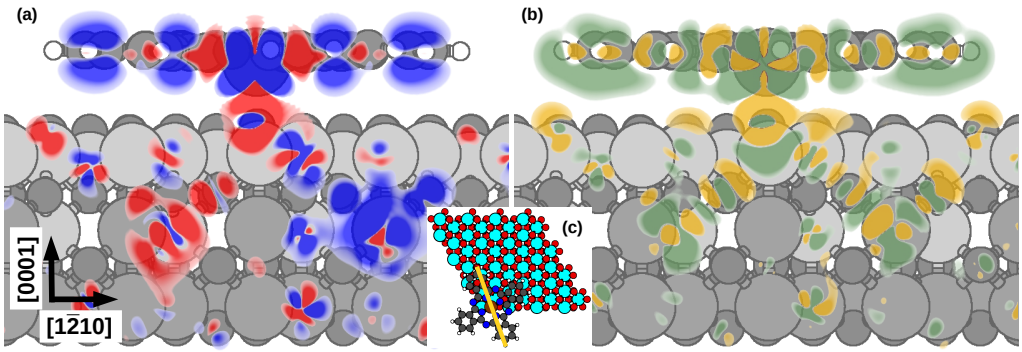


Figure 7.5 Side-view of the spin density (a) and charge density variations (b) of the minimum energy adsorption configuration with respect to the isolated systems (full-color regions correspond to values whose modulus exceeds 0.001 Å$^{-3}$). The vertical plane on which data is shown is marked in yellow in panel (c) and forms a small angle ($10°$) with respect to the $[01\bar{1}0]$ direction). Red/blue: increase/decrease in spin density; yellow/green: increase/decrease in electron density.

the molecule only superficially, in reality from a side-view large variations can be observed propagating inside the substrate. The variations inside the substrate are of those atoms along the crystalline directions. In particular, the two sub-surface Cr atoms along the diagonals in Fig. 7.5 increases in their magnetic moment modulus by $0.7\mu_B$ and in their electronic charge by $0.187$. These two atoms are linked to the surface ones by super-exchange mechanisms through the O-down atoms. The directionality of the results derives from the alignment of one of the N-Fe-N axes of the molecule with an high-symmetry surface azimuth. Looking instead at the molecule in Fig. 7.6-(d) it is clear a significant movement of electronic charge towards the substrate ($1.5\ e^-$), with the noticeable exception for the two pyrrolic N atoms along the $[1\bar{2}10]$ direction. Analogous variations in the magnetic moments can be observed in Fig. 7.6-(b). The spin-crossover effect lifts the degeneracy of the molecule in the Fe $d_{xz}$ and $d_{yz}$ orbitals, making the Jahn-Teller distorsion not anymore needed; in fact, the molecule reacquires its $D_4$ symmetry, electronically (in the Fe d orbitals) and structurally (the ratio between the Fe-N asymmetric bonds changes from $0.1\%$ to $0.03\%$).

## 7.4 Optical properties

Analogously to the other spinterfaces, at this point, we can discuss the optical properties of FePc/$Cr_2O_3$(0001) in the minimum adsorption configuration, reporting the 2D polarizability in Fig. 7.7, for the adsorbed system and for the pristine one. The intensities of the three spectra are scaled by the same factor, chosen so to normalize the transition at $1.5$ eV in the free molecule to unity. While the free molecule onset is at lower energies than the pristine substrate one, the full system one is at lower energies than the free molecule one, underlining a significant hybridization between the molecule and the substrate, as already notice in the PDOS Fig. 7.4.

In the lower inset of Fig. 7.7, the relative intensities of the transitions are reported in red, for the two spin-channels, normalized with respect to the maximal one at $\simeq 1.4$ eV

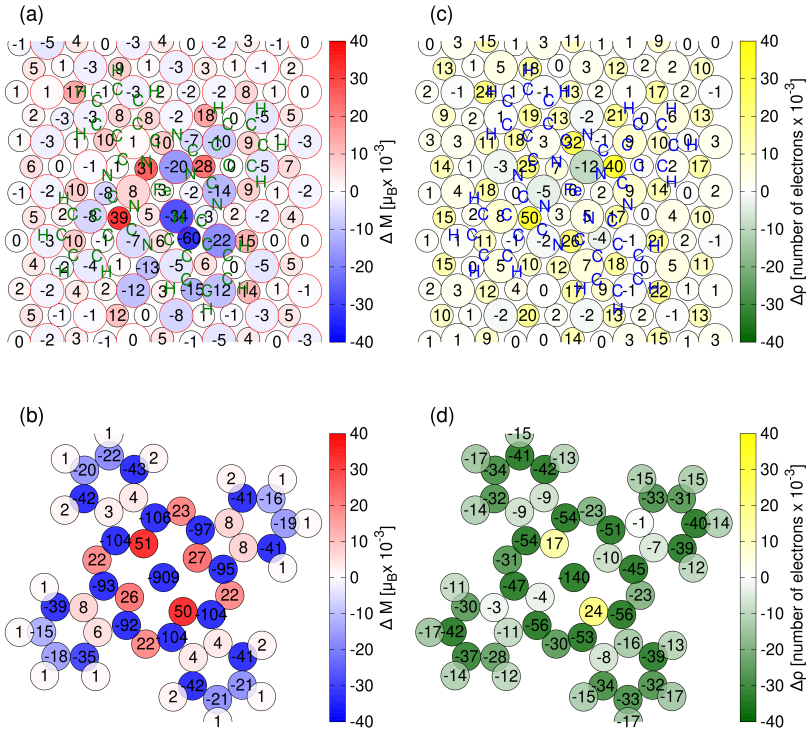


Figure 7.6 Variations in the atomic magnetic moments for FePc/$Cr_2O_3$(0001) with respect to the isolated systems: (a) on the surface and (b) on the molecule. (c), (d) Corresponding variations in the electron population (positive = increase in electron population). The colour of the circles contour is associated with the spin of the pristine substrate atoms: red = majority spin magnetization; blue = minority spin magnetization. The position of molecule atoms is marked by green letters in panels (a) and (c).

(bins with relative intensity lower than 10% of the maximal one are omitted). In the upper inset of Fig. 7.7, the molecular contributions (Yellow) to the valence and conduction states $P_b^{(v/c)}$ are reported for each transition (Purple).

The first part of the spectrum $< 1.4$ eV is characterised mainly by small intensity transitions in the spin-up channel, which are responsible for the little bump at $\simeq 1$ eV. These transitions are by valence substrate states to conduction states of mainly molecular nature. For what concern the spin-down channel, in fact, only a small transition appears at 1 eV, which can be related, instead, to a molecule HOMO/HOMO-1 to substrate conduction/conduction+1 pair. The rest of the peaks at higher energies have major intensities, but only little molecular contributions.

As in the other spinterface, we can take a look at the relative heights of the valence and conduction states contributing to the transitions. In the spin-up channel, the peaks at energies $[0.08 - 1.08)$ eV are characterized by transitions mainly from the sub-surface tri-layer $z^{(v)} = 5.0 \pm 0.4$ Å to underneath the molecule $z^{(c)} = 9 \pm 1$ Å, while the peaks at higher energies involve atoms in the middle and bottom tri-layers. In the spin down-

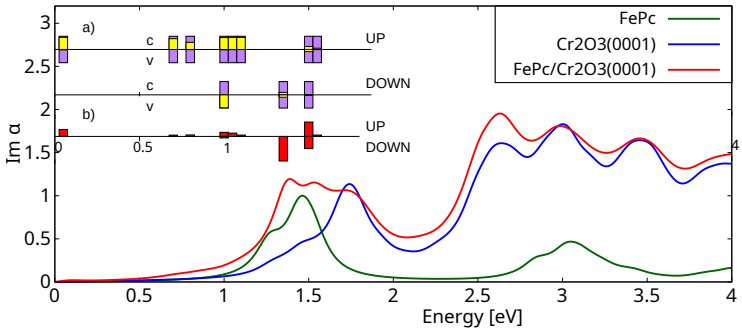


Figure 7.7 Optical absorption spectra (independent particle): polarizability of $Cr_2O_3(0001)$ (blue), $FePc/Cr_2O_3(0001)$ (red), and an FePc molecular layer such as in $FePc/Cr_2O_3(0001)$ (green). The arbitrary units are chosen by normalizing the molecular peak at $\simeq$1.5 eV (green line) to 1. The transitions are broadened by $0.01$ eV. Bottom inset (b): the intensities (red) of the main transitions contributing to the $FePc/Cr_2O_3(0001)$ spectrum in the spin-up (top) and spin-down (bottom) channels, normalized with respect to the largest one at $\simeq$1.4 eV. Only values greater than $5\%$ are shown. Top inset (a): the percentage of projection of the respective valence(bottom)/conduction(top) level on the molecule (yellow), characterizing the main transitions.

channel, the peaks at energies $1.37$ and $1.53$ eV involve, instead, the bottom tri-layers.

To note that the similar small peaks, in the two spin-channels, respectively at $1.08$ eV and $1.03$ eV, are characterized by transitions to/from the molecule $z_{c/v} = 10.7 \pm 1$ Å to/from the bottom tri-layers $z^{(v),(c)} = 2.5 \pm 0.1$ Å.

## 7.5 Multiple molecular configurations at the ground-state

In studying spinterfaces and analyzing them the possibility of multiple minima energetically and structurally nearby appeared. This has required a particular care into looking at the DFT results, and more than once to perform many more self-consistent calculations than we could have expected. This variety of local minima is due to the impressive number of degrees of freedom and it is mostly related to the high perturbability of the molecular states.

As an example, here we report the PDOS in Fig. 7.8 of a configuration of the FePc $/Cr_2O_3(0001)$ O-terminated spinterface, that is structurally very similar to the O-up $30^\circ$ AF reported above, but differs in terms of molecular states in proximity of the Fermi energy. It has an adsorption energy of $-4.611$ eV, that is $0.033$ eV bigger than the minimal one. We will indicate this configuration O-up $30^\circ$ AF - bis.

As underlined above, a noticeable difference between the electronic structures of the two configurations O-up $30^\circ$ AF and O-up $30^\circ$ AF-bis, respectively in Fig. 7.4 and in Fig. 7.8, is the switching of the two molecular levels HOMO and LUMO in the two spin-channels. This change, affecting the molecular magnetism, leaving untouched the Fe

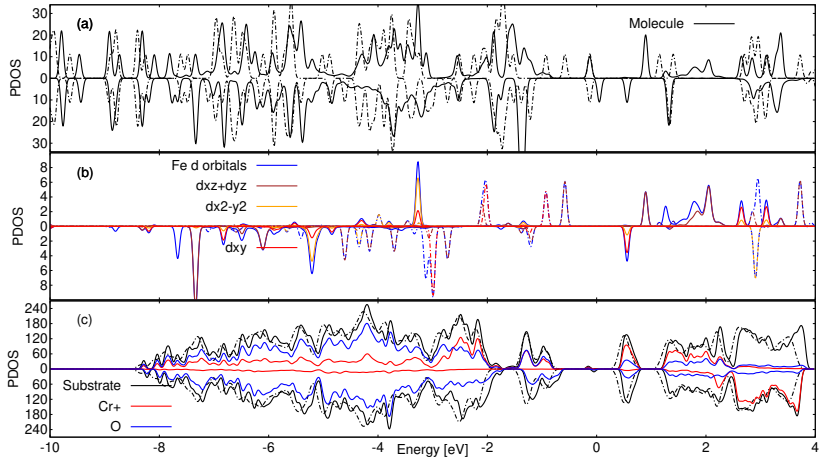


Figure 7.8 O-up 30° AF-bis: Electronic PDOS of FePc/$Cr_2O_3$(0001), summed over: (a) all molecule atoms; (b) Fe d-orbitals; (c) substrate atoms. Substrate color codes: black = all substrate atoms; red = Cr atoms of one spin component ("Cr+", $d$ orbitals); blue = all O atoms. Solid/dash-dotted lines indicate adsorbed and gas phase molecules or pristine substrate, respectively. Negative spin components are shown as negative values. All values in states/eV/cell.

atom magnetic moment, has significant effects on the optical spectra at low adsorption energies.

## 7.6 Conclusions

From these studies of the FePc adsorption on the $Cr_2O_3$(0001) in its O-terminated configuration, it emerges the tendency of the molecule to dispose its molecular axis along the crystalline directions of the substrate. Looking at the spin density and charge density variations, moreover, it emerges a coupling at the interface, local at the surface, but that spreads deeply into the substrate. This suggests that this spinterface, with respect to the one of the former Chapter 6, affects deeply the magnetic state of the substrate. This, however, does not translate in high intensity transitions of substrate/molecular character at low energies of the optical spectrum.

# Part V
# Fe-phthalocyanine on NiO

CHAPTER 8

# Fe-phthalocyanine on NiO(001)

In the following chapters, we study the spinterface problem of FePc/NiO(001), from a DFT perspective and from an Heisenberg perspective. The main motivation for this theoretical study that so far does not have an experimental counterpart, is to consider a simpler substrate compared to the previous ones and to understand which are the effects on the magnonic properties due to the molecule adsorption.

From the DFT perspective, the FePc lies flat and binds through the O surface atom to the Ni underneath, in an anti-ferromagnetic super-exchange fashion. Moderate changes to the magnetic structure of the components and charge displacement are shown. Optical spectra show transitions mainly of molecular character and a reduction of the adsorption onsets. The possibility of a coupling of the optical excitation with the system spin properties is investigated. The majority of the results in this chapter have been published in Ref. [119].

From the Heisenberg perspective, the small variations in the exchange couplings of the substrate due to the molecule adsorption, confirm a weak coupling at the spinterface. This translates into small effects on the magnonic properties. Although this spinterface does not show large enough coupling between the molecule and the substrate, it helps us to better understand this interesting physical problem.

## 8.1 Computational details

We evaluate the ground state of the FePc/NiO(001) spinterface and its properties using DFT in a plane-wave basis set, with U and VdW corrections, as already pointed out in the Section 2.4. The values considered, $U_{Ni} = 4.0$ eV and $U_{Fe} = 5.0$ eV, were chosen following the literature so as to optimize the electronic properties (density of states) of the localized orbitals for the isolated systems [119, 146, 155, 156]. The substrate is modeled with a slab that includes $3$ NiO layers. Equilibrium geometries are obtained through a structural optimization of the molecule and of the top two layers of the substrate. In the same way, the optical spectra are obtained and analyzed following what already pointed out in Section 2.4.

## 8.2 Adsorption configurations

The adsorption of FePc on NiO(001) is studied considering the surface supercell $((6,0),(3,3))$, built from the surface magnetic unit cell, as depicted in Fig. 8.1.

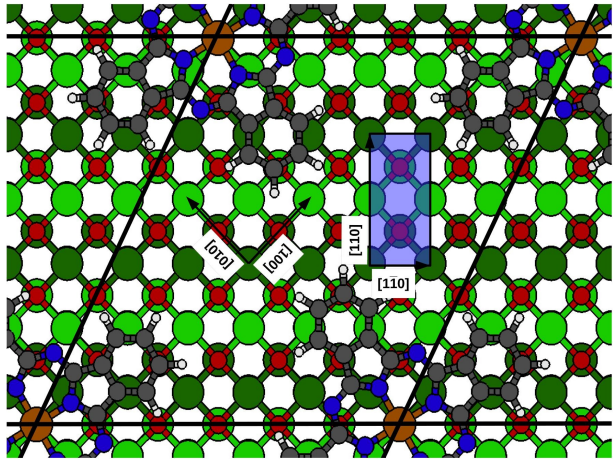


Figure 8.1 Surface supercell adopted for the calculations (black line), having epitaxy matrix $((6,0),(3,3))$ with respect to the surface primitive cell of antiferromagnetic NiO(001) (shaded-blue). Color scheme as follows. Light and dark green: Ni atoms, according to their magnetization; Red: O; Brown: Fe; Blue: N; Dark-gray: C; Light-gray: H.

Table 8.1 Adsorption energy for FePc/NiO(001) as a function of adsorption site and optimized angle, for FM and AF orientation of the Fe spin with respect to underlying Ni. Values in eV.

| Site | Angle | $E_{\text{ads}}^{\text{FM}}$ | $E_{\text{ads}}^{\text{AF}}$ | $E_{\text{ads}}^{\text{AF}} - E_{\text{ads}}^{\text{FM}}$ |
|---|---|---|---|---|
| Ni | $0°$ | -4.39 | -4.21 | 0.18 |
| Ni | $22°$ | -4.38 | -4.59 | -0.21 |
| Ni | $45°$ | -4.34 | -4.51 | -0.16 |
| O | $0°$ | -4.57 | -4.70 | -0.13 |
| O | $31°$ | -5.12 | -5.18 | -0.05 |
| O | $45°$ | -4.68 | -4.71 | -0.03 |

The FePc overlayer with a distance between the molecules of $17.68$ Å, compared with the experimental results of Pc molecules on Al(001) substrate ($\simeq 14$ Å)[154], can be considered diluted. The smallest distance between the H atoms of two molecules is $5.73$ Å, so no interaction between the molecule is expected.

Different adsorption configurations have been considered, these are distinguished by the adsorption center of the Fe atom, i.e. Ni or O, the molecular orientation, i.e. the angle between the N-Fe-N axis and the substrate crystalline direction $[1\bar{1}0]$, and the two possible magnetic configurations of the molecule with respect to the Ni under the Fe atom, in case of adsorption on top of O, the Ni beneath the O atom is considered (assuming that the super-exchange interaction mediated by the O atom is stronger than the exchange interaction at the surface). We call the spin configuration with Fe and Ni spin in the same direction ferromagnetic (FM), while the one with the two in the opposite direction antiferromagnetic (AF). The optimized structures are reported in Figure 8.2, while the respective adsorption energies are reported in Table 8.1.

The O configurations are generally lower in energy than Ni ones. The two O config-

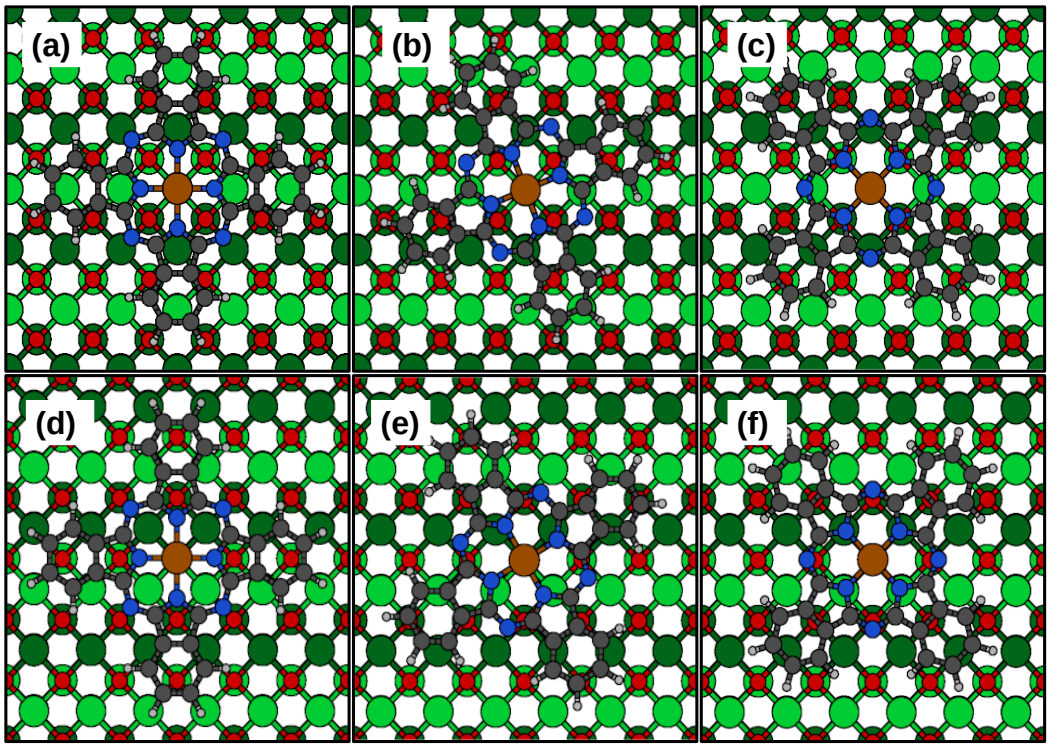


Figure 8.2 Optimized geometries for FePc/NiO(001) on a Ni site (a-c) and on a O one (d-f), with optimized azimuthal angle (see text) equal to $0°$ (a,d), $22°$ (b), $30°$ (e), and $45°$ (c,f). Color scheme as in Fig. 8.1.

urations at $0°$ and at $45°$ have similar energies, while the one at $30°$ have a lower energy (this configuration is obtained starting from an O configuration at $22.5°$). The difference in energy can be explained by a weak interaction between the imide N atoms and the surface Ni atoms, and a stronger interaction between the phenyl-rings C atoms and the surface Ni atoms, as can be seen by the spin-density differences in Fig. 8.6. The real-space spin density difference is obtained as

$$\Delta\mu(\boldsymbol{r}) = \mu_{\text{molecule+substrate}}(\boldsymbol{r}) - (\mu_{\text{molecule}}(\boldsymbol{r}) + \mu_{\text{substrate}}(\boldsymbol{r})) \tag{8.1}$$

where $\mu(\boldsymbol{r}) = \sum_{nk}(|\psi_{nk\uparrow}(\boldsymbol{r})|^2 - |\psi_{nk\downarrow}(\boldsymbol{r})|^2)$ and respectively the spin density of the adsorbed system (molecule+substrate) and the ones of the isolated systems (molecule and substrate) are considered.

In the Ni configurations, and the larger distance of the molecule from the substrate and the fact that the bonding between the phenyl-rings C atoms and the Ni atoms is not particularly favoured in none of the configurations, the effects of the rotation are less evident. From the perspective of the molecular magnetic ordering, while gloabally an anitferromagnetic ordering is shown, there is an exception for the Ni configuration at $0°$. While the Fe position can partially explain the magnetic behaviour, the rotation of

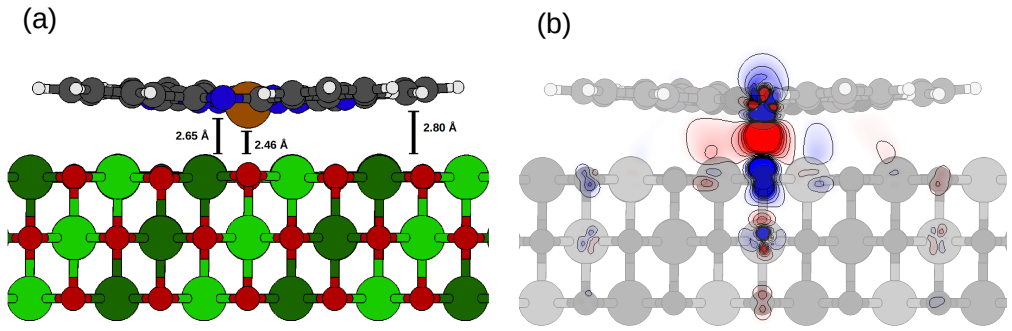


Figure 8.3 (a) Side view of FePc/NiO(001) in the most stable (O $30^\circ$ AF) configuration and height over the surface of the Fe atom and of the average CHN atoms (Å). (b) Spin-density variation (red: increase; blue: decrease); isolines in the range from -0.02 to 0.02 $\text{Å}^{-3}$.

the molecule seems to have a major role. The JT distorsion in the molecule makes the Fe atom more sensible to the pyrrolic N atoms along one direction with respect to the one in the other, with the consequence that the O and Ni adsorption configurations are not completely symmetric with respect to the two directions for what concern the pyrrolic N atoms. Moreover, the O and Ni configurations at $0^\circ$ have the imide N atoms over equally magnetized Ni atoms, taking into account a possible super-exchange mechanism through the O atoms. The major proximity of the Fe atom to a pair of oyrrolic N atoms, and the fact that N atoms couple antiferromagnetically with the Fe atom, could partially explain the different magnetic behaviour of the molecule.

Coming to the adsorption geometries, in the Ni configurations the molecule atoms are located at a distance of $2.92 \pm 0.01$ Å (average height) from the top surface layer at the different angles, while in the O configurations the lowering of the Fe atom, cause a deformation of the molecule, with a reduction of the distance. This is quite significant in the minimum adsorption energy configuration, the O configuration at $30^\circ$, where the Fe atom sits at $2.64$ Å, pulling the N atoms at $2.65$ Å. The distance between the Fe and O atom, approaches the typical bonding length in bulk FeO ($2.14$ Å). The weak JT distorsion ($0.1\%$) is preserved in the adsorption.

## 8.3 Electronic properties

Focusing on the most stable configuration, we study its electronic properties looking at the PDOS in Fig. 8.4. The deep states of the molecule, in the free-standing configuration and in the adsorbed one, are aligned; in fact, these states are untouched by the adsorption.

The adsorption reduces the bandgap of the substrate, as the LUMO of the molecule lies within it, Tab. 8.2. A type II interface is then formed, as the HOMO of the molecule lies within the valence band of the substrate. Generally, the adsorption shifts and hybridizes the molecular levels. In particular, looking at the d orbitals in Fig. 8.5, between the ones towards the surface the $d_{xz}$ and $d_{yz}$ are the most affected ones: underlining a

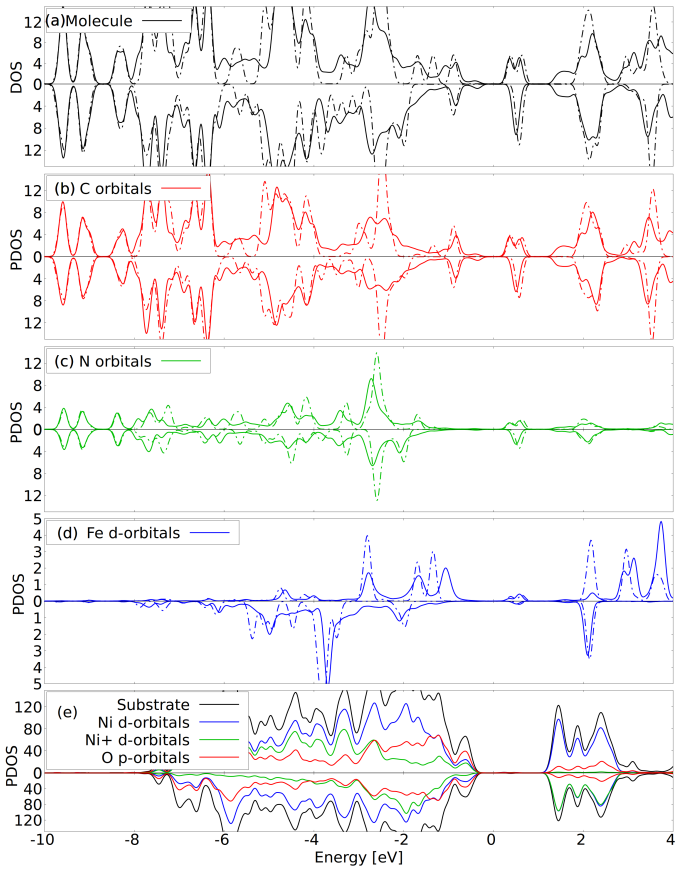


Figure 8.4 Electronic PDOS of FePc/NiO(001), summed over: (a) all molecule atoms; (b) C; (c) N; (d) Fe; (e) substrate atoms. Substrate color codes: Black: all substrate atoms; Blue: all Ni atoms ($d$ orbitals); Green: Ni atoms of one spin component ("Ni+", $d$ orbitals); Red: O atoms ($p$ orbitals). Solid/dash-dotted lines indicate adsorbed and gas phase molecules, respectively. Negative spin components are shown as negative values. All values in states/eV/cell. The deep states of the molecule, in the free-standing configuration and in the adsorbed one, are aligned; in fact, these states are untouched by the adsorption.

strong coupling between the molecule and the surface.

## 8.4 Magnetic properties

In Fig. 8.6, the variations in the magnetic moments and in the electronic charge at the surface and in the molecule are reported. The effects of the adsorption are mainly localized at the surface, as can be observed in the spin density difference in Fig. 8.6. A lowering of the magnetic moments can be observed, of the Ni below the center of the molecule up to about $30\times10^{-3}\mu_B(\simeq 2\%)$, as well as of the O up to about $10\times10^{-3}\mu_B$, with the exception

Table 8.2 Electronic gap of the full FePc/NiO(001) system in comparison to free FePc and to the clean NiO(001) surface.

| System | Spin channel | Gap (eV) |
|---|---|---|
| free FePc | up | 1.27 |
| free FePc | down | 1.46 |
| FePc/NiO(001) | up | 0.69 |
| FePc/NiO(001) | down | 0.80 |
| NiO(001) | up/down | 1.80 |

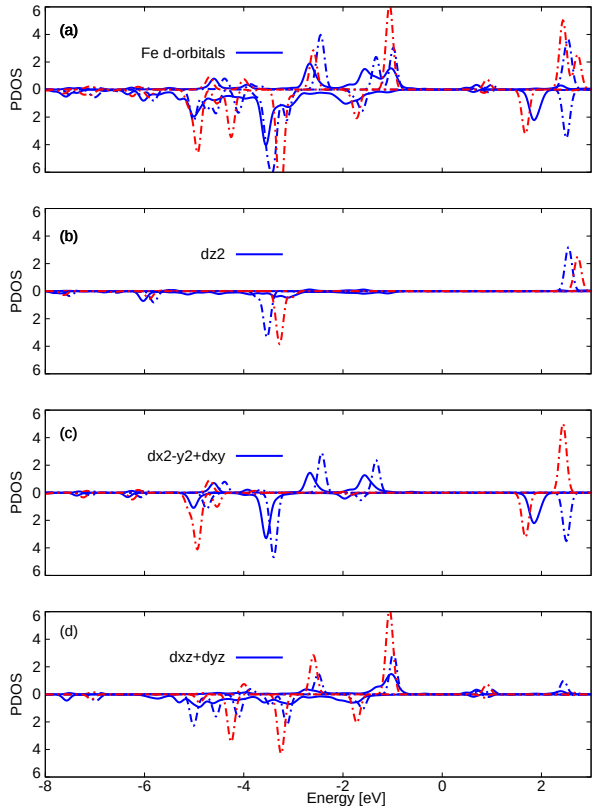


Figure 8.5 Electronic PDOS on the Fe atom in FePc/NiO(001). (a) all $d$ orbitals; (b) projected on $d_{z^2}$; (c) $d_{x^2-y^2} + d_{xy}$; (d) $d_{xz} + d_{yz}$. Blue solid/dash-dotted lines indicate adsorbed and gas phase ($D_{2h}$) molecules, respectively. Red dash-dotted lines indicate the gas phase molecule in the $D_{4h}$ configuration. Negative spin components are shown as negative values. All values in states/eV/cell.

of the one under the Fe atom up to about $30 \times 43^{-3}\mu_B$. The loss of electronic charge of the O atoms under the molecule, and correlated decrease of the magnetic moment, can be justified as the attempt of the O to establish a simil super-exchange coupling between the Ni atoms underneath and the molecule atoms above; while this is quite evident for

the O atom under the Fe atom, for the other O atoms is less clear, as not all the molecule atoms acquire electronic charge as the Fe atom. In other words, we could say that the molecule with its de-localized $\pi$ orbitals, reduces the local magnetic moments of the TM atoms, with consequent decrease of the super-exchange mechanism mediated through the O atoms, and consequent decrease of the hopping electrons trough the O atoms.

Looking at the molecule, instead, the main changes occur at the Fe atom, with a reduction of its magnetic moment by $40 \times 10^{-3}\mu_B$ (from $-2.17$ to $-2.13\mu_B$). Overall, the net molecule magnetic moment changes from $-2.00$ to $-1.95\mu_B$, excluding the Fe magnetic moment from $0.172$ to $0.176\mu_B$. While the electronic charge variations of the molecule partially remind the JT distorted molecule, the magnetic moments variation do not; probably, due to the fact that the substrate does not preserve magnetically this symmetry.

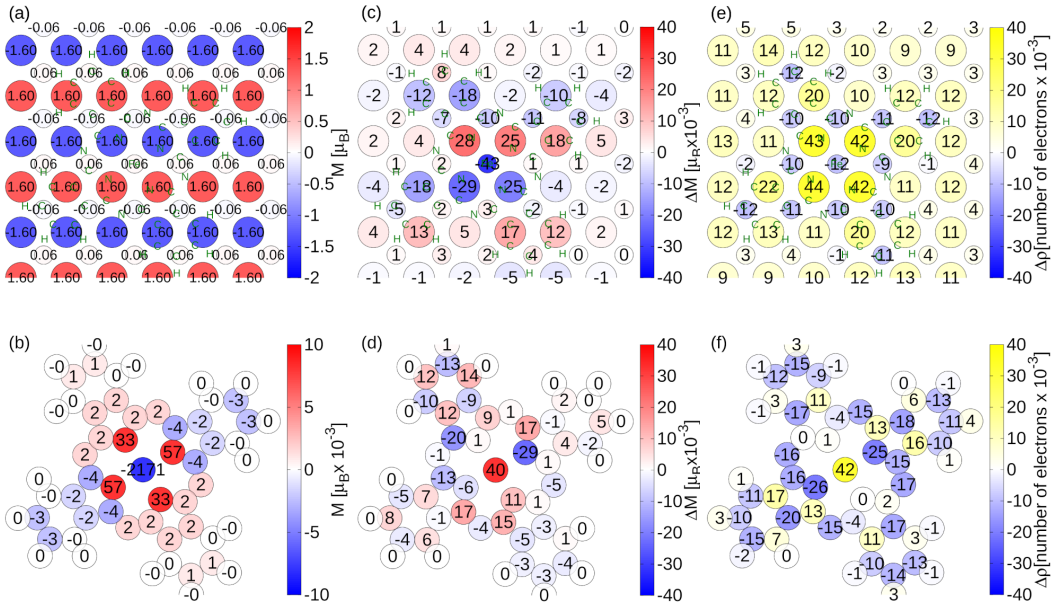


Figure 8.6 Values of the atomic magnetic moments for the clean surface NiO(001) (a) and the isolated molecule FePc (b); variations in the atomic magnetic moments for FePc/NiO(001), with respect to the isolated systems, on the surface (c) and on the molecule (d). Corresponding variations in the electron density (e)-(f) (positive=increase in electron population). The position of molecule atoms is marked by green letters in panels (a), (c), and (e).

## 8.5 Optical properties

In Fig. 8.7 the spectra for the FePc/NiO(001) system are reported, and compared with the ones of the pristine NiO(001) and of the free-standing FePc layer. A set of peaks for the adsorbed system appears below the adsorption edge both of NiO and of FePc. These peaks are, then, related to the interface states, i.e. to effects of hybridization between the molecular orbitals and the substrate orbitals.

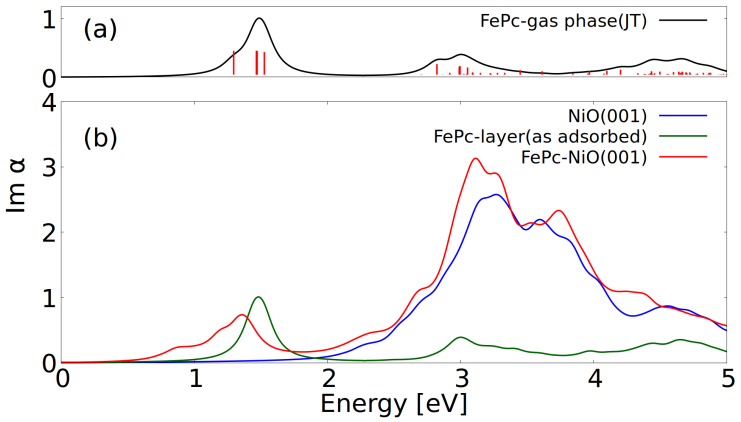


Figure 8.7 Optical absorption spectra (independent particle): (a) gas-phase molecular polarizability (black line) and respective transitions (red sticks); (b) polarizability of: NiO(001) (blue), FePc/NiO(001) (red), and FePc-layer as in FePc/NiO(001) (green). The two spectra (a) and (b) are separately normalized to the molecular peak at $\approx 1.5$ eV. Spectra are broadened by $0.1$ eV.

Contributions at $1.19, 1.33, 1.36$ and $1.41$ eV are identifiable to the ones of the free-molecule. These are transition from FePc valence states of C nature to conduction states of C nature ($62\%$), N nature ($25\%$) and Fe nature ($2\%$ in the minority spin channel and $1\%$ in the majority spin channel). Thus, the Fe atom fills its empty orbitals $d_{xz}/d_{yz}$ in the minority spin channel; this is not a proper light induced spin-crossover. This would occur if the involved levels in the optical transitions had a major d contribution: as in the case of the $d_{z^2}$ or $d_{x^2-y^2}$ orbitals, which, however, are at higher energies.

Additionally, to the free-molecule-like peaks, in the adsorbed system a secondary peak appear around $0.9$ eV that is $\simeq 1/7$ as intense as the other peaks. This is given by transition where the conduction state corresponds to the molecular LUMO/LUMO+1 orbitals, while the valence state is mostly of substrate origin, corresponding to the interface state at $\simeq 0.4$ eV in the PDOS 8.4.

## 8.6 Conclusions

We identified the minimum adsorption configuration as the one with the Fe atom over an O atom and the molecule lying flat over the surface. We noticed that certain angles of the molecule enable a molecular lock-in into the surface, with the Fe atom pulled towards the O atom. The O atom favors a super-exchange coupling between the Fe atom and the Ni beneath. This coupling is underlined by the spin density difference and the hybridization of the d orbital of the Fe pointing towards the surface. Local variations of the magnetization and of the charges are observed at the bonding point. A reduction of the Ni magnetic moments is observed due to charge transfer from the O atoms of the surface.

For what concern the optical spectra, the breaking of the spin degeneracy, which in principle would allow a spin excitation through light, is observed as in the other spinterfaces. However, in this case, the valence states and conduction states are molecular